Equilibrium and kinetic studies on complex formation and decomposition and the movement of Cu^{2+} metal ions within polytopic receptors

.

Carmen E. Castillo,[a] Jorge González-García,[b] José. M. Llinares,[b] M. Ángeles Máñez,[a] Hermas R. Jimenez,[b] Enrique García-España*[b] and Manuel G. Basallote.*[a]

[a]*Departamento de Ciencia de los Materiales e Ingeniería Metalúrgica, Facultad de Ciencias, Universidad de Cádiz, Polígono Rio San Pedro, s/n, Puerto Real, 11510 Cádiz, Spain. E-mail: manuel.basallote@uca.es*

[b]*Instituto de Ciencia Molecular, Departamento de Química Inorgánica, Universidad de Valencia, C/Catedrático José Beltrán 2, 46980, Paterna, Valencia, Spain. E-mail: enrique.garcia-es@uv.es*

Supplementary Material include:

Table S1.- Logarithms of the stability constants for the formation of mononuclear, binuclear and trinuclear complexes of Cu^{2+}: **L3**, **L4**, **L5** and **L6** calculated in 0.15 mol dm^{-3} NaCl at 298.1 ± 0.1 K

Figure S1.- Distribution diagrams of the species for the **L2**/Cu^{2+} systems as a function of pH in aqueous solution in 0.15 mol dm^{-3} at 298.1 K; [**L2**] = 1×10^{-3} M. (a) [Cu^{+2}] = 1×10^{-3} M, (b) [Cu^{+2}] = 2×10^{-3} M and (c) [Cu^{+2}] = 3×10^{-3} M.

Figure S2.- Distribution diagrams of the species for the **L1**/Cu^{2+} systems as a function of pH in aqueous solution in 0.15 mol dm^{-3} at 298.1 K; [**L1**] = 1×10^{-3} M. (a) [Cu^{+2}] = 1×10^{-3} M, (b) [Cu^{+2}] = 2×10^{-3} M and (c) [Cu^{+2}] = 3×10^{-3} M.

Figure S3. Distribution diagrams of the species for the **L2**/Cu^{2+} systems as a function of pH in aqueous solution in 0.15 mol dm^{-3} at 298.1 K; [**L2**] = 1×10^{-3} M. (a) [Cu^{+2}] = 1×10^{-3} M, (b) [Cu^{+2}] = 2×10^{-3} M and (c) [Cu^{+2}] = 3×10^{-3} M.

Figure S4.- 400 MHz proton NMR spectra in D_2O at 298 K and pH=7.2 of $[Cu_3\mathbf{L1}]^{6+}$. In the downfield region, the intensity of the spectrum is multiplied by five. The asterisks mark the residual solvent and impurity signals (*, H_2O; **, HOD).

Figure S5.- Plot of the dependence on the acid concentration of the observed rate constant for the first kinetic step in the formation process of Cu^{2+} and **L2** in 1:1 (triangles) and 2:1 (circles) Cu:**L2** molar ratio ([NaCl]= 0.15 mol dm^{-3}, 298.1 K).

Figure S6.- Distribution diagrams for the protonation of **L1** (a) and **L2** (b).

Table S1.- Logarithms of the stability constants for the formation of mononuclear, binuclear and trinuclear complexes of Cu^{2+}: **L3**, **L4, L5** and **L6** calculated in 0.15 mol dm^{-3} NaCl at 298.1 ± 0.1 K

Reaction [a]	*L3*[c]	*L4*[d]	*L5*[d]	*L6*[e]
$3H + Cu + L \leftrightarrows CuH_3L$				
$2H + Cu + L \leftrightarrows CuH_2L$				
$H + Cu + L \leftrightarrows CuHL$		*24.28(2)*	*22.65(2)*	
$Cu + L \leftrightarrows CuL$	*17.78(2)*[b]	*20.43(3)*	*19.65(4)*	*22.6(1)*
$Cu + L + H_2O \leftrightarrows CuL(OH) + H$		*9.42(3)*		
$2H + 2Cu + L \leftrightarrows Cu_2H_2L$				
$H + 2Cu + L \leftrightarrows Cu_2HL$				
$2Cu + L \leftrightarrows Cu_2L$				
$2Cu + L + H_2O \leftrightarrows Cu_2L(OH) + H$				
$3Cu + L \leftrightarrows Cu_3L$				
$CuH_2L + H \leftrightarrows CuH_3L$				
$CuHL + H \leftrightarrows CuH_2L$				
$CuL + H \leftrightarrows CuHL$		*3.85(3)*	*3.00(2)*	
$CuL + H_2O \leftrightarrows CuL(OH) + H$		*-11.01(3)*		
$Cu_2LH + H \leftrightarrows Cu_2H_2L$				
$Cu_2L + H \leftrightarrows Cu_2HL$				
$CuL + Cu \leftrightarrows Cu_2L$				
$Cu_2L + H_2O \leftrightarrows Cu_2L(OH) + H$				
$Cu_2L + Cu \leftrightarrows Cu_3L$				

[a] Charges omitted. [b] Values in parenthesis show standard deviation in the last significant figure. [c] Taken from ref.11. [d] Taken from ref. 9. [e] Taken from ref. 10

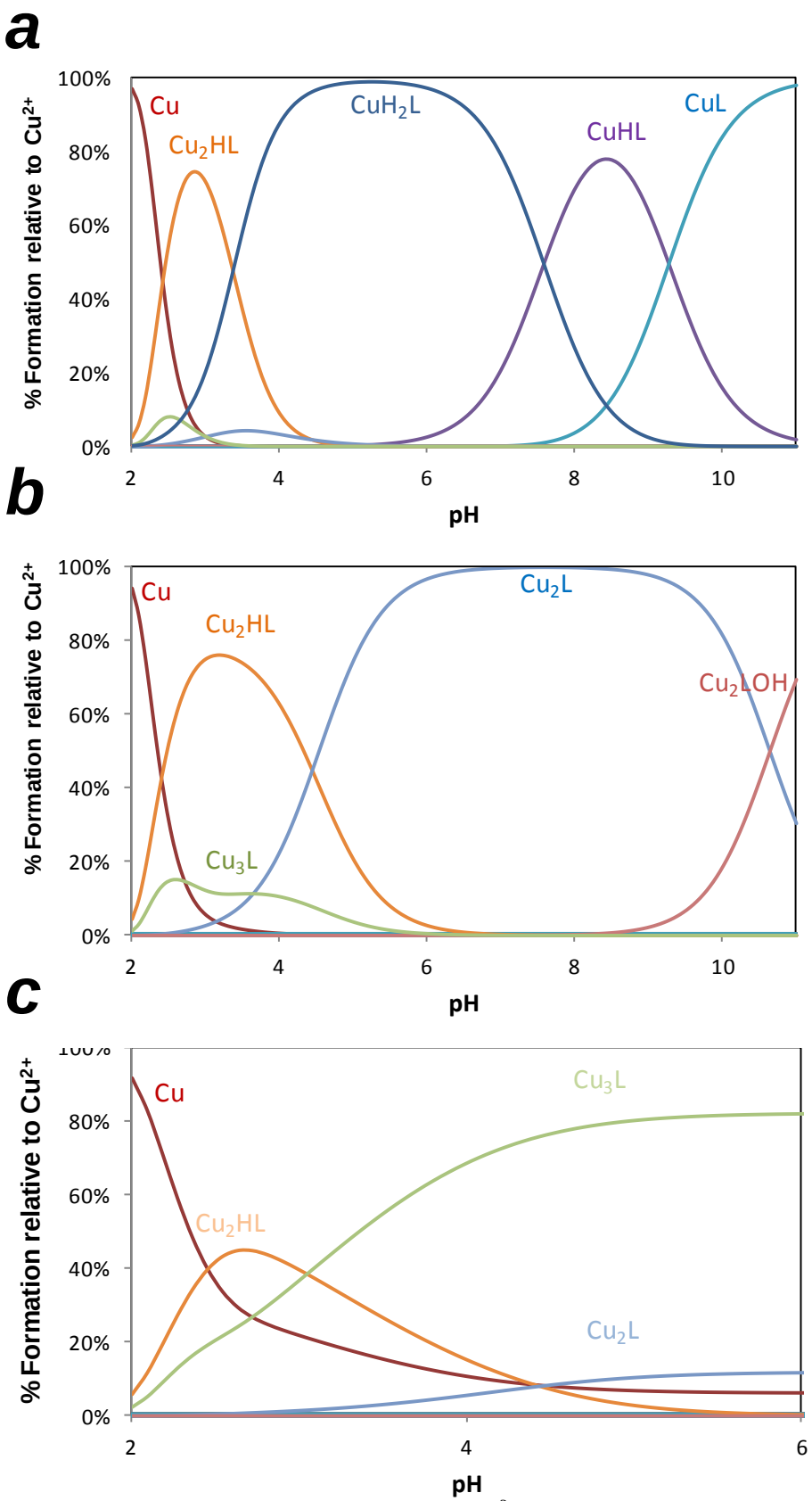

Figure S1. Distribution diagrams of the species for the **L2**/Cu^{2+} systems as a function of pH in aqueous solution in 0.15 mol dm^{-3} at 298.1 K; [**L2**] = 1×10^{-3} M. (a) $[Cu^{+2}] = 1 \times 10^{-3}$ M, (b) $[Cu^{+2}] = 2 \times 10^{-3}$ M and (c) $[Cu^{+2}] = 3 \times 10^{-3}$ M.

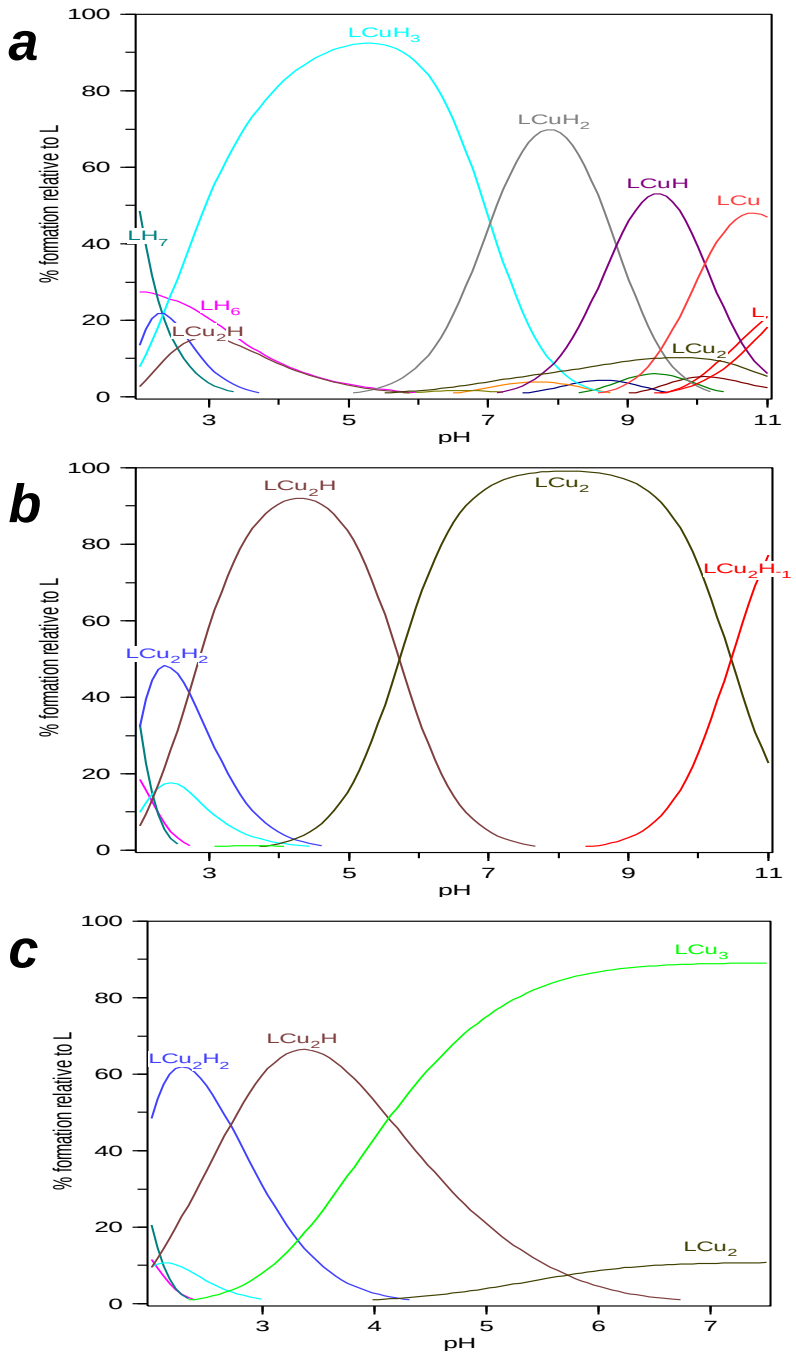

Figure S2. Distribution diagrams of the species for the **L1**/Cu^{2+} systems as a function of pH in aqueous solution in 0.15 mol dm^{-3} at 298.1 K; [**L1**] = 1×10^{-3} M. (a) [Cu^{+2}] = 1×10^{-3} M, (b) [Cu^{+2}] = 2×10^{-3} M and (c) [Cu^{+2}] = 3×10^{-3} M.

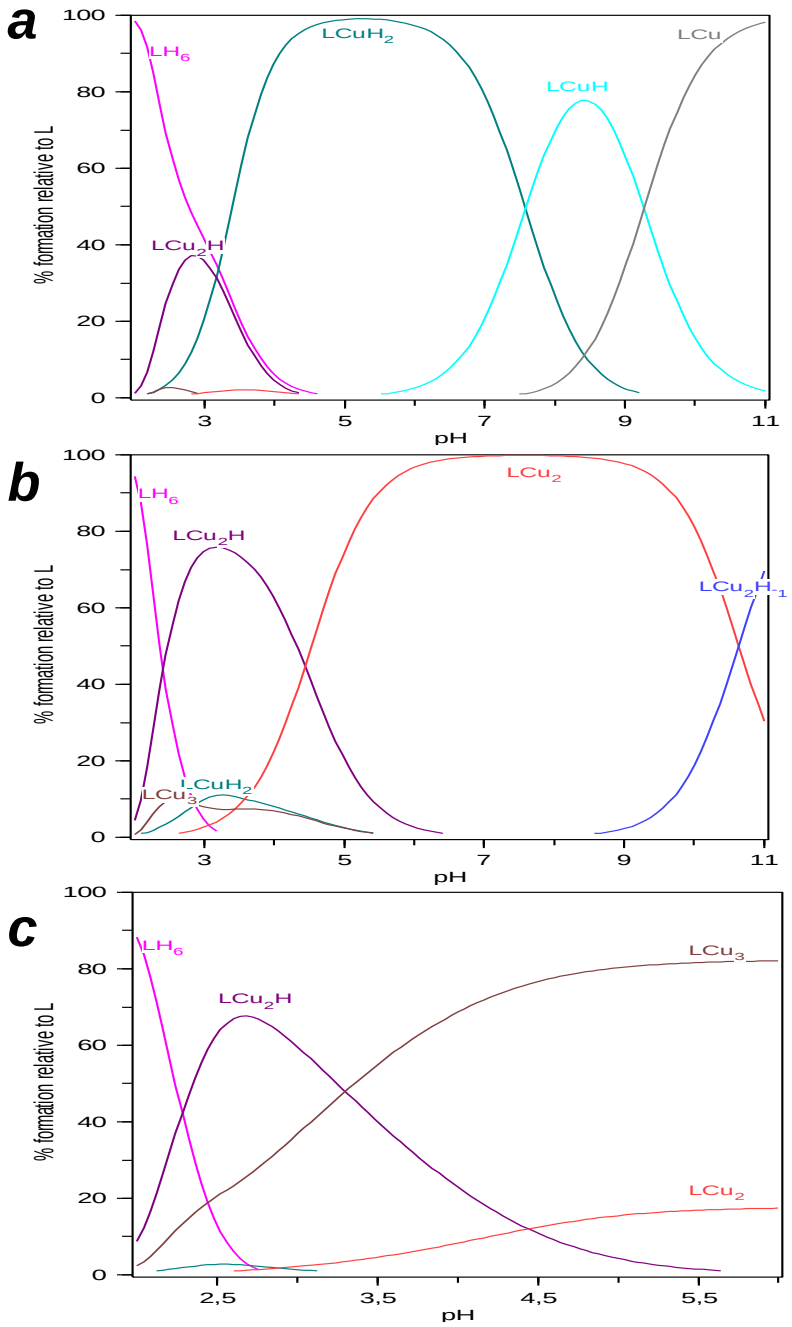

Figure S3. Distribution diagrams of the species for the **L2**/Cu^{2+} systems as a function of pH in aqueous solution in 0.15 mol dm^{-3} at 298.1 K; [**L2**] = 1×10^{-3} M. (a) [Cu^{+2}] = 1×10^{-3} M, (b) [Cu^{+2}] = 2×10^{-3} M and (c) [Cu^{+2}] = 3×10^{-3} M.

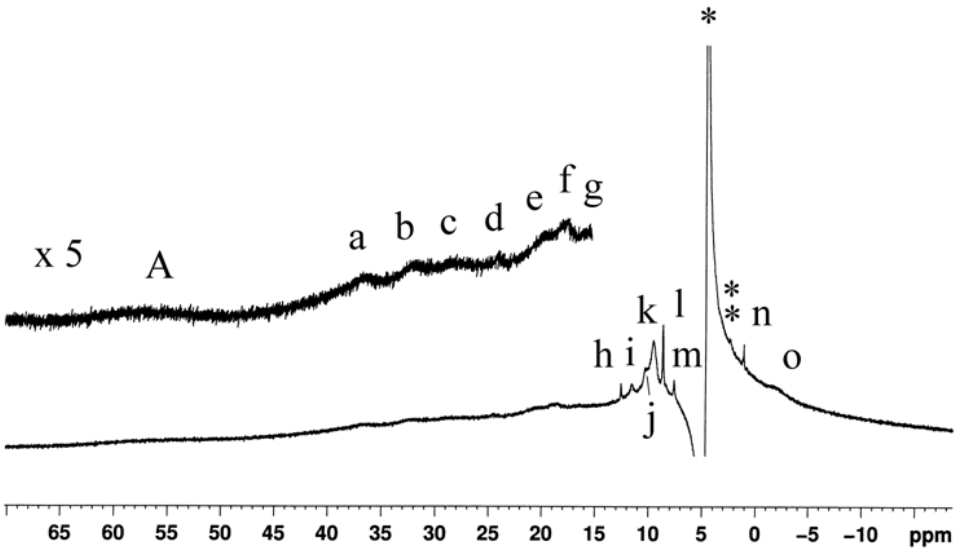

Figure S4.- 400 MHz proton NMR spectra in D_2O at 298 K and pH=7.2 of $[Cu_3\mathbf{L1}]^{6+}$. In the downfield region, the intensity of the spectrum is multiplied by five. The asterisks mark the residual solvent and impurity signals (*, H_2O; **, HOD).

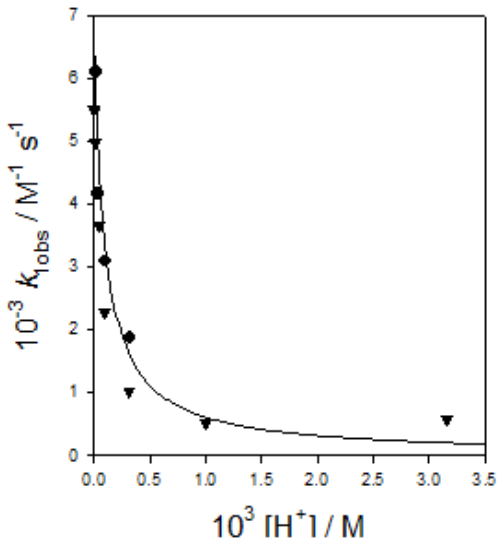

Figure S5. Plot of the dependence on the acid concentration of the observed rate constant for the first kinetic step in the formation process of Cu^{2+} and **L2** in 1:1 (triangles) and 2:1 (circles) Cu:**L2** molar ratio ([NaCl]= 0.15 mol dm^{-3}, 298.1 K).

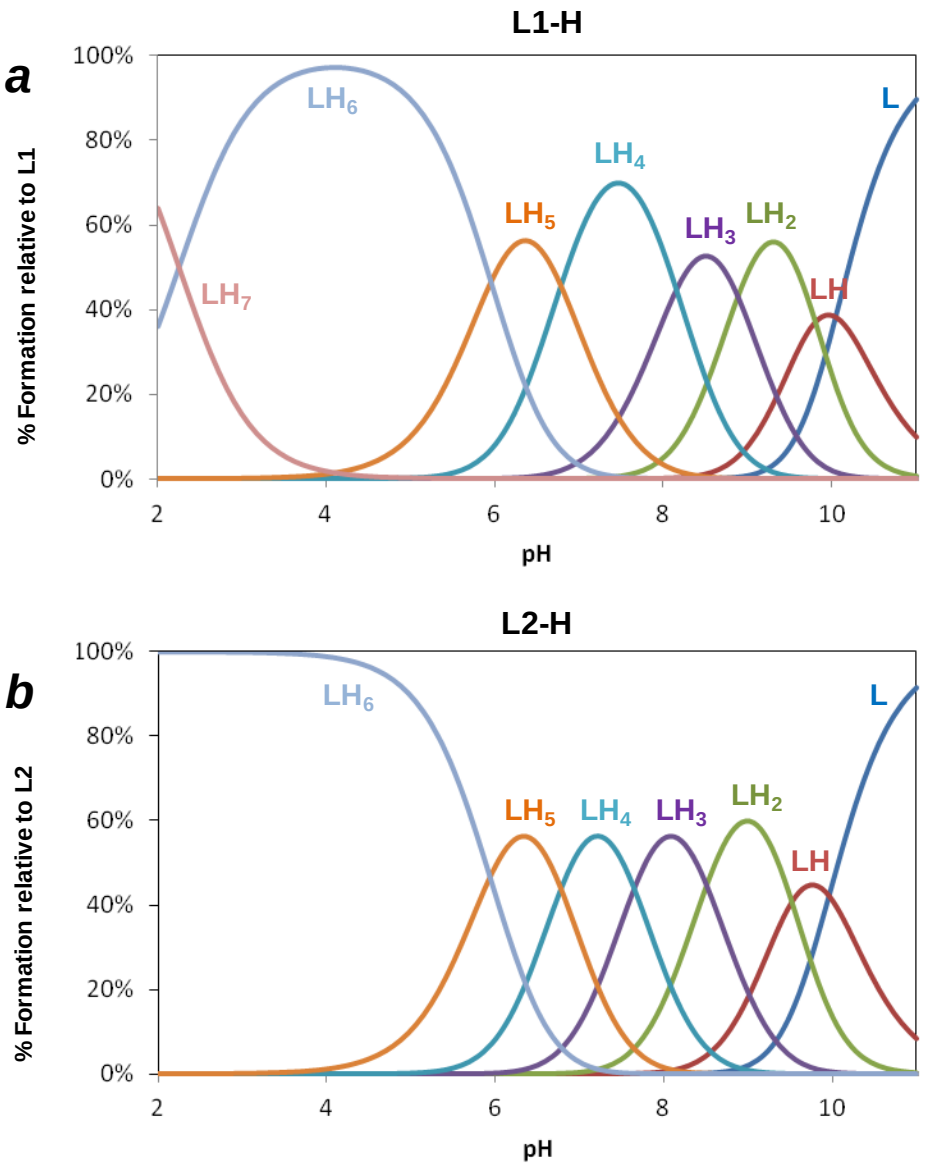

Figure S6. Distribution diagrams for the protonation of **L1** (a) and **L2** (b).